

Graded Roll-to-Roll Slot Die Coating for High-Throughput Catalyst Layer Studies

George Pätzold,^[a, b] Maximilian Maier,^[a, b] Lukas Lötttert,^[a, b] Anna T. S. Freiberg,^[a, b] Simon Thiele,^[a, b] and Dominik Dworschak^{*[a]}

Fuel cells play a key role in the energy transition to renewable resources. Many of these systems are based on substrates coated with thin layers containing catalyst, ionomer or support material like carbon. In order to experimentally define the optimal catalyst layer configuration, one must do step-by-step variations of its components. Currently this must be done in several single coating experiments. Here we present a tabletop roll-to-roll (R2R) slot die coating setup for producing wet film graded catalyst layers for high-throughput loading studies. In the presented work we perform a loading study for proton exchange membrane fuel cell (PEMFC) cathodes where all

investigated loadings result from one single coating. The wet film thickness is measured during the continuous coating process via in-line confocal sensors and is correlated by area X-ray fluorescence (XRF) scans. Small sections of the graded catalyst layer coatings were tested in a full cell PEMFC with a 5 cm² active area. The known loading dependency of PEMFC performance was shown and compared to previous loading studies. The results show the successful fabrication of the graded layer which can be used for both, to facilitate materials development and to increase cell performance in stacks.

Introduction

Proton exchange membrane fuel cells (PEMFCs) play a key role in the energy transition to renewable resources.^[1] A lot of different parameters influence the electrochemical performance of catalyst layers for PEMFC, so many studies have focused on determining the optimal platinum-on-carbon based catalyst layer so far. There are several studies varying the carbon support type,^[2,3] the ionomer to carbon (I/C) ratio^[4,5] and the overall platinum loading^[6–8] in the catalyst layer in an experimental or simulative way.^[9,7] Additionally, the variation of the platinum loading can be done via varying the wet film layer thickness during the coating process, via dilution of the platinum on carbon with pure carbon^[6] or via variation of the overall solid content in the catalyst ink. Furthermore, one can

use different solvents for the catalyst inks depending on the coating method^[10,11] used.

Former parameter studies were usually done manually with laboratory-based, established coating methods such as spray coating,^[3,5] wire rod,^[12,11] doctor blade,^[3] screen printing.^[4,13] For all of those methods a new coating must be conducted when coating a catalyst layer with a new parameter set.

One solution for speeding up parameter studies can be found in the field of printed photovoltaics. Via the in-line mixing of the active materials in a roll-to-roll (R2R) slot die coating process in-plane gradients can be produced.^[14] In that way many different composed samples covering a huge parameter space can be manufactured in a short amount of time with just one coating.

Ayoub et al. suggested that in-plane gradients can be a powerful tool for PEMFC catalyst layers too.^[15] Nevertheless, in-plane gradients were only used to enhance the performance of single cells^[16] so far. To the best of our knowledge, there are no studies using in-plane gradients for catalyst layer optimization. Furthermore, all reported in-plane graded catalyst layers have been an assembly out of several discreet loading regimes. A linear gradient of, for instance the catalyst loading has not been reported so far for PEMFCs.

Considering the demand of new materials^[17] for enhancing the performance of PEMFCs and other electrochemical systems such as PEM water electrolysis^[18] or alkaline systems,^[19] there is a need of a material and time efficient method for screening of catalyst layer parameters. The goal is to bring new materials faster and more efficiently into application than in the conventional way via established lab-based coating methods.

In this work we introduce a setup based on a tabletop R2R coater for fast and material efficient production of in-plane gradients. As a first study we varied the volume flow into the slot die head to produce an in-plane loading gradient for a

[a] G. Pätzold, M. Maier, L. Lötttert, A. T. S. Freiberg, Prof. Dr. S. Thiele, Dr. D. Dworschak
Electrocatalytic Interface Engineering
Helmholtz-Institute Erlangen-Nürnberg for Renewable Energy (IET-2), Forschungszentrum Jülich
Cauerstraße 1, Erlangen, 91058, Germany
E-mail: d.dworschak@fz-juelich.de
Homepage: <https://www.hi-ern.de/en/research/electrocatalysis/high-throughput-electrochemistry>

[b] G. Pätzold, M. Maier, L. Lötttert, A. T. S. Freiberg, Prof. Dr. S. Thiele
Department of Chemical and Biological Engineering
Friedrich-Alexander-Universität Erlangen-Nürnberg
Cauerstr. 1, Erlangen, 91058, Germany

Supporting information for this article is available on the WWW under <https://doi.org/10.1002/celc.202400688>

© 2025 The Authors. ChemElectroChem published by Wiley-VCH GmbH. This is an open access article under the terms of the Creative Commons Attribution License, which permits use, distribution and reproduction in any medium, provided the original work is properly cited.

platinum based PEMFC ink. The wet film thickness was measured via in-line installed confocal distance sensors and the relative platinum distribution was determined via X-ray fluorescence spectroscopy (XRF). Finally, we conducted full cell PEMFC measurements at different positions of the gradient at the corresponding platinum loadings.

Experimental

Catalyst ink preparation – For the catalyst ink we used 40%_{wt} platinum on a vulcan carbon support (Tanaka TEC10V40E) and as an ionomer Nafion™ D2020 (Chemours) with an I/C ratio of 0.65. As solvents we used 1-propanol (88%_{wt} of liquid phase) and H₂O. The total amount of catalyst powder was 10.7%_{wt}. The ink was dispersed in a 30 ml HDPE bottle with 100 ZrO₂ beads (5 mm diameter) for 18 h with 60 rpm via roller milling. The same catalyst ink was used for both the graded cathode and the non-graded anode coating.

Coating process – The coating was conducted on an InfinityPV LR2RC1500 tabletop coater with a total length of 1.5 m. As a coating substrate we used 100 µm thick virgin PTFE foil with a width of 140 mm obtained from High-Tech-Flon. The slot die head, which was obtained from InfinityPV, had a coating width of 50 mm and a 250 µm thick shim shaping the opening of the slot die.

All coatings were carried out with a web tension of 3 MPa and a 150 µm coating gap. The graded cathode was coated with a web speed of 0.15 m min⁻¹. The coating was conducted with the following protocol for the volume flow of the syringe pump. At the beginning of the experiment the ink volume flow was held constant at 0.85 ml min⁻¹ for 2 min for providing stable coating conditions. Subsequently, the volume flow was decreased linearly to 0 ml min⁻¹ within 6 min. Together with the given web speed and the width of the slot die head a linear decrease of the film thickness from 113 µm to 0 µm equation (1) within 90 cm of the web can be calculated. In practice, after 70 cm of coating at around 0.19 ml min⁻¹ and a calculated resulting wet film thickness of 25 µm visible inhomogeneities of the coated catalyst layer occur, so that it is not usable for electrochemical measurements. The usable 70 cm of the graded coating contains a Pt loading gradient from slightly over 0.3 mg_{Pt} cm⁻² down to slightly less than 0.1 mg_{Pt} cm⁻² (compare Figure 3). Once the coating is done and has passed the confocal sensors the web is stopped manually. Subsequently, the catalyst layer is dried at lab temperature (22.5 ± 0.5 °C) until it is visibly dry, so no solvent could be seen in the catalyst layer anymore and it looked dull. Afterwards the coated PTFE was cut into 20 cm pieces and put into a lab oven (Binder) for 2 h at 70 °C for assuring a full removal of any solvents out of the catalyst layer. All experiments were repeated three times. SEM pictures of the dried catalyst layer can be found in the supporting information (S4).

The distance between the position of the confocal wet film thickness measurement and the roller nips is about 1.4 m, so that the coating length of 1.2 m (2 min constant plus 6 min graded coating at a constant web speed of 0.15 m min⁻¹) fits in that space.

The anode catalyst layer was coated with the same parameters as the graded cathode, but with a constant volume flow (0.6 ml min⁻¹) and a web speed of 0.3 m min⁻¹ resulting in a wet film thickness of 40 µm and a loading of 0.1 mg_{Pt} cm⁻².

In-line wet film thickness measurement – For the in-line measurement of the wet film thickness, we used confocal sensors (CL-3000, Keyence) with a CL-L030 head and a resolution of 0.25 µm. The

measurement was performed with a scan rate of 1 kHz corresponding to one measured point every 2.5 µm at a web speed of 0.15 m min⁻¹.

XRF measurement – For the XRF measurements we used a Bruker M4 TORNADO with a spot diameter of 20 µm. Two different measurement modes were used. For validation of the confocal sensors, we used a line scan in the middle of the coating at the same positions where the confocal sensors measured the wet film thickness. Each measured datapoint had a distance of 2 mm to the next one. In this work that method will be referred to as XRF line scan. In the other mode we measured the area of the full length of the graded coating in a width of 2 cm in the middle of the coating to generate an areal information of the coating. All points in the measured grid had a distance of 2 mm to each other in length and width. In the following this will be referred to as XRF areal scan. For recording the XRF spectra we conducted the measurement for each point with 50 kV and 600 µA and a measurement time of 1 s. For determining the qualitative platinum loading of the catalyst layer, the platinum peak integrals of the fluorescence spectra were analysed and will be referred to as XRF Pt Intensity in this work. A representative XRF spectrum is displayed in the supporting information (S6).

It is important to point out, that the displayed XRF Pt intensities only show a relative change of platinum within the catalyst layer and that they are only valid for the catalyst layer system in this study. For a detailed quantification of the loading via XRF and accounting for changes in the matrix a calibration with pellets of the metal in a matrix would be needed, which will be important especially for more complex samples.

CCM manufacturing – For manufacturing the catalyst coated membrane (CCM) we used a die cutting tool to cut out 5 cm² square samples for both cathode and anode. Both electrodes were hot pressed on a Nafion™ 211 (Chemours) membrane with a hot press (LAB LINE P200S, COLLIN Lab & Pilot Solutions GmbH). For hot pressing the CCM and PTFE were sandwiched between two square 25 cm² pressure pads (PACOPADS™ #5500, Pacothane Technologie) for assuring equal pressure distribution and Kapton sheets between the CCM and the pressure pads on each side to avoid CCM contamination. The gravimetric loading was determined via weighing the coated 5 cm² cut out PTFE sheet before and after decal transfer. The measured loadings for each single CCM can be found in the supporting information (S3). The hot pressing was conducted with the following parameters: hold for 60 s at 120 °C and a pressure of 0.5 MPa, linear increase of the temperature within 150 s up to 155 °C and then holding 155 °C at a pressure of 1.2 MPa for another 240 s.

Full cell testing – For full cell testing we used gas diffusion layers (GDL) from Freudenberg with the specification H14CX653 on both electrodes. As gaskets we used glass fiber reinforced PTFE with a thickness to provide a cell compression of 20%. The thickness of the CCM and membrane was measured four times at different positions with a dial gauge (Mitutoyo Absolute) and averaged. The GDL and gaskets were measured three times at different positions with a micrometre gauge and averaged. The membrane electrode assembly was then brought into a Scribner cell fixture with an active cell area of 5 cm² and a single-channel, multi-serpentine graphite flow field.

For the electrochemical measurements we used a Scribner 850e test station with backpressure system and a VSP-300 Biologic potentiostat. The break-in procedure and the recording of the I–V-curve were conducted at a cell temperature of 80 °C, a relative humidity of 95 % and a relative backpressure of 50 kPa. The anode

was fed with pure hydrogen with a flow rate of 0.25 ml min^{-1} and the cathode with synthetic air with a flow rate of 0.75 ml min^{-1} .

The break-in procedure was conducted via a voltage hold at 0.6 V for 45 min, then going back to OCV for 5 min and a voltage hold at 0.85 V for 10 min. This protocol was repeated 12 times for providing a full break-in of the cell.^[12] For recording the I–V-curve we went to a voltage hold at 0.75 V right after the break-in. After going back to OCV we conducted current holds of 0.1 A, 0.25 A, 0.5 A, 1 A, 2.5 A, 3.75 A, 5 A, 6.25 A, 7.5 A, 8.75 A, 10 A each for 10 min. For the I–V-curve the mean voltage value of the last 30 s at each current step (incl. OCV) was calculated. For HFR determination we conducted GEIS measurements at each current step with an amplitude of 10% of the absolute current going from 100 kHz to 10 Hz. The measured data were fitted with an equivalent circuit model consisting of an inductor, a charge transfer transmission line model^[20] and a resistor representing the HFR.

For additional cell characterization we measured the hydrogen crossover from anode to cathode, the electrical short, the protonic sheet resistance^[21] and the electrochemical surface area via cyclic voltammetry. Measurement conditions and results can be found in the supporting information (S3)

Results and Discussion

R2R Setup

Figure 1 shows the schematic drawing of the coating setup used for manufacturing of the graded catalyst coating on the PTFE foil. In the following, the PTFE foil is referred to as web. The two main rolls (unwinder and rewinder) are keeping the web under tension and the drive applies a constant web speed. For providing enough friction urethane rubber roller nips (Misumi – RONSS30-15-50) were pressed on the driven roll. The slot die head was fed via a tubing and a syringe pump, of which the pump speed can be adjusted during the coating process.

$$d_{\text{wet}} = \frac{\dot{V}_{\text{ink}}}{W \cdot v_{\text{web}}} \quad (1)$$

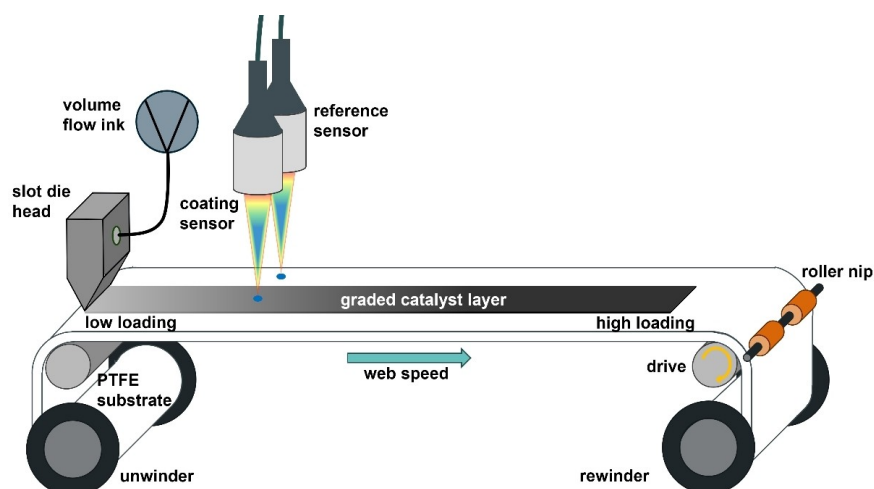


Figure 1. Schematic drawing of the tabletop R2R coater upgraded with confocal sensors for wet film thickness measurements. Via a modification of the volume flow a gradient in wet film thickness of the catalyst ink is applied on the PTFE substrate

The gradient of the loading results from a graded wet film thickness d_{wet} . This is realized via the modification of the volume flow of the ink \dot{V}_{ink} into the slot die head. According to equation (1) d_{wet} is directly proportional to \dot{V}_{ink} and additionally dependent on the two parameters width of the slot die head ($W = 50 \text{ mm}$) and velocity of the web ($v_{\text{web}} = 0.15 \text{ m min}^{-1}$), which were both held constant during all experiments. A visualisation of the coating process and the main following analysis steps are shown in the supporting information (S5)

For an in-line control of the wet film thickness of the graded coating the setup is equipped with two confocal distance sensors with a resolution of $0.25 \mu\text{m}$. One sensor is directly measuring the height differences in the middle of the coating and the other one operates as a reference sensor for the correction of web tilting perpendicular to the moving direction of the web. The sensors are mounted with a centre point distance of 34 mm next to each other. The measured profile from the reference sensor is then subtracted from the profile of the coating sensor. The distance between the coating head and the confocal sensors is 51 mm, so the coating needs 20 s to move from the slot die head to the in-line thickness measurement. Height differences because of drying during this time were found to be neglected.

Dependency of Wet Film Thickness and XRF Signal

As discussed above, the wet film thickness of the coating process is in-line monitored via two confocal distance sensors. For verification of the confocal thickness measurement the XRF Pt Intensity is measured in the middle of the coating along the web at the same line where the confocal sensor measures the wet film thickness.

The XRF intensity value for Pt gives semi-quantitative information about the Pt content in the catalyst layer. Presuming a homogeneous dispersion of the catalyst ink, it is expected to correlate linearly with the wet film thickness of the whole coating. Figure 2 shows the plot of the wet film thickness

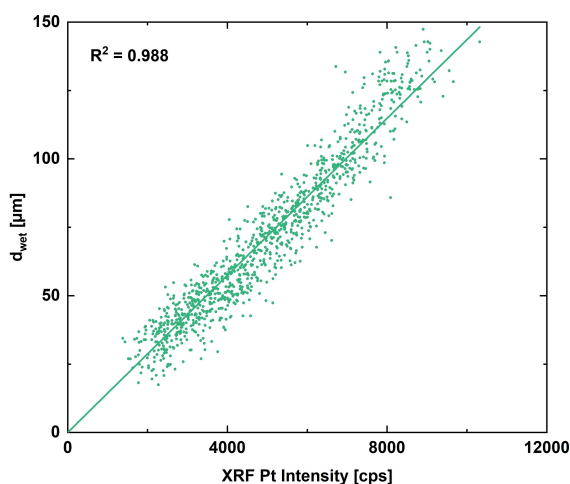


Figure 2. Correlation of the measured wet film thickness over the corresponding XRF Pt Intensities measured with line scanning of the coating including all three repetitions of the experiment showing the expected linear dependency.

over the corresponding XRF Pt Intensities at the different discrete along the web positions in the middle of the coating for all three repetitions of the experiment. As expected, the two values correlate linearly with each other with an R^2 value of 0.988 and a slope A of $0.0143 \mu\text{m cps}^{-1}$ according to equation (2) with a standard error of $4.88 \cdot 10^{-5} \mu\text{m cps}^{-1}$.

$$d_{\text{wet}} = A \cdot \text{XRF Pt Intensity} \quad (2)$$

This shows that the XRF Pt Intensity and the measured wet film thickness are directly linearly correlating with each other. Therefore, the areal XRF Pt Intensity can be used to calculate the areal wet film thickness. The measured linear decrease of the wet film thickness and XRF Pt Intensity in the middle of the coating for all three experiments can be found in the supporting information (S1)

Dependency of Wet Film Thickness, Areal XRF and Gravimetric Loading

XRF can be used to make area scans of the catalyst layer. As described above the XRF Pt Intensity is directly proportional to the wet film thickness according to equation (2). This stems from the correlation of the Pt areal loading with the wet film thickness.^[4] As the former can gravimetrically only be determined at discrete positions, the XRF intensity is a suitable tool to analyse the gradient as such.

The upper graph of Figure 3 shows the calculated wet film thickness according to equation (1) and the correspondent measured thickness in the middle of the coating for one representative single experiment (all repetitions are shown in Figure S2). The measured wet film thickness matches with the linearly decreasing calculated values. The slightly higher wet film thickness between 0 mm and 100 mm at an expected wet film thickness of over $100 \mu\text{m}$ is resulting from non-equally

spread ink over the whole width of the slot die head due to high volume flows.

The graph in the middle of Figure 3 shows the mean value of the areal XRF scan with the width of 2 cm with the standard deviation stemming from the single pixels over the coating width shown as an error band. The standard deviation of the Pt XRF Intensity does not rise above 850 cps. According to equation (2) this corresponds to a standard deviation in wet film thickness of not more than $10 \mu\text{m}$ around the mean value perpendicular to the coating direction. Just as the XRF value in the middle of the coating the areal XRF values are also decreasing linearly. As described earlier the whole coating is cut into 20 cm pieces of length after coating to make it processable in the oven and XRF. The coating at the cutting edges at the positions 100 mm, 300 mm and 500 mm are damaged due to the cutting process, so those values are not representative for the coating itself and were thus removed from the dataset.

The lower graph shows the positions of the Pt loadings $0.3 \text{ mg}_{\text{Pt}} \text{ cm}^{-2}$, $0.2 \text{ mg}_{\text{Pt}} \text{ cm}^{-2}$ and $0.1 \text{ mg}_{\text{Pt}} \text{ cm}^{-2}$, which are determined gravimetrically. The graphs for the two other repetitions of the experiment can be found in the supporting information (S2). Out of all three experiments with the given decrease of volume flow from 0.85 ml min^{-1} to 0 ml min^{-1} within 6 min in the described setup induces a decrease of loading of $36 \cdot 10^{-3} (\text{mg}_{\text{Pt}} \text{ cm}^{-2}) \text{ cm}^{-1}$ with a standard deviation of $3.6 \cdot 10^{-3} (\text{mg}_{\text{Pt}} \text{ cm}^{-2}) \text{ cm}^{-1}$. Therefore, it can be assumed, that the Pt loading on one single cut out square electrode with an area of 5 cm^2 is sufficiently homogeneous for a full cell test representative of the individual loadings.

Figure 4 shows the wet film thickness and XRF Pt Intensity over corresponding loading out of three repetitions of the experiment. For comparability, the wet film thickness is displayed as the mean value in a length of 2.2 cm of the cut-out electrode. XRF Pt Intensity is the mean value of an area of 5 cm^2 at the position where the electrode was cut out.

The wet film thickness and XRF Pt Intensity scale linearly with the corresponding loading with an R^2 value of 0.997 and

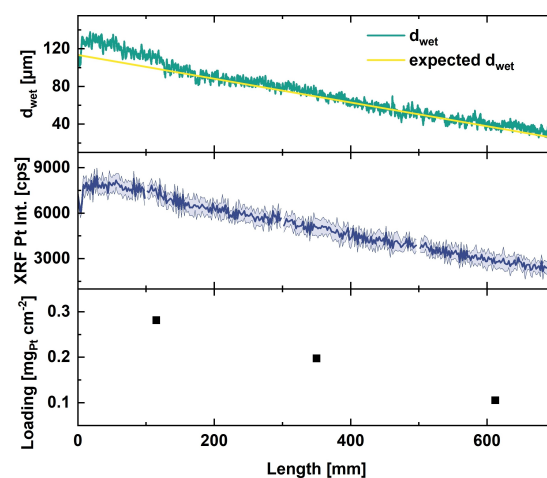


Figure 3. Wet film thickness, XRF Pt Intensity on a stripe of 2 cm width and the Pt loading of a 5 cm^2 electrode of the coated gradient. The light purple colour around the Pt XRF Intensity graph shows the standard deviation in width direction.

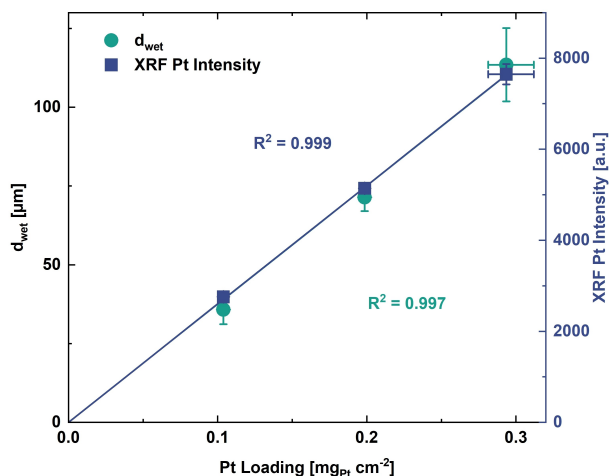


Figure 4. Wet film thickness and XRF Pt Intensity over the corresponding areal loading of the electrode. The error bars in Y-direction show the standard deviation of the averaged data points for wet film thickness and XRF Pt Intensity. The error bars in X-direction show the min-max range of the measured loading.

0.999 respectively. This shows, that both the XRF Pt Intensity and the wet film thickness can be used for predictions of the gravimetric loading.

Electrochemical Measurement

For electrochemical characterisation three different cathode loadings of all three coating repetitions were tested in a PEMFC full cell with an anode loading of $(0.11 \pm 0.01) \text{ mg}_{\text{Pt}} \text{ cm}^{-2}$. The anodes for the cell tests are produced with the same ink and coating method like the cathodes, but with constant wet film thickness of $40 \mu\text{m}$.

Figure 5 shows the measured I–V-curves with the standard deviation shown as error bars after the break-in. As already reported in literature, the performance improvement from $0.1 \text{ mg}_{\text{Pt}} \text{ cm}^{-2}$ cathode loading to $0.2 \text{ mg}_{\text{Pt}} \text{ cm}^{-2}$ is greater than the improvement from $0.2 \text{ mg}_{\text{Pt}} \text{ cm}^{-2}$ to $0.3 \text{ mg}_{\text{Pt}} \text{ cm}^{-2}$. At low loadings the performance is limited, due to mass transport limitations which scale inversely with reduced available platinum surface.^[22] Those are occurring because of limited accessibility of the active sites for oxygen at low loadings, longer diffusion length through the ionomer^[6] and an additional contact resistance between the platinum catalyst and the ionomer.^[22] Due to higher mass transport limitations because of the thickness of the electrodes the performance does improve only slightly when increasing the loading further to $0.3 \text{ mg}_{\text{Pt}} \text{ cm}^{-2}$.^[6]

The HFR value remains in a range between $40 \text{ m}\Omega \text{ cm}^2$ and $60 \text{ m}\Omega \text{ cm}^2$ for all tested current densities. For all three loadings the HFR decreases with higher current due to better protonic conductivity due higher humidification of the membrane because of water formation.^[23,24] At current densities bigger than 1250 mA cm^{-2} , the HFR increases again due to anode dry-out.^[23,24]

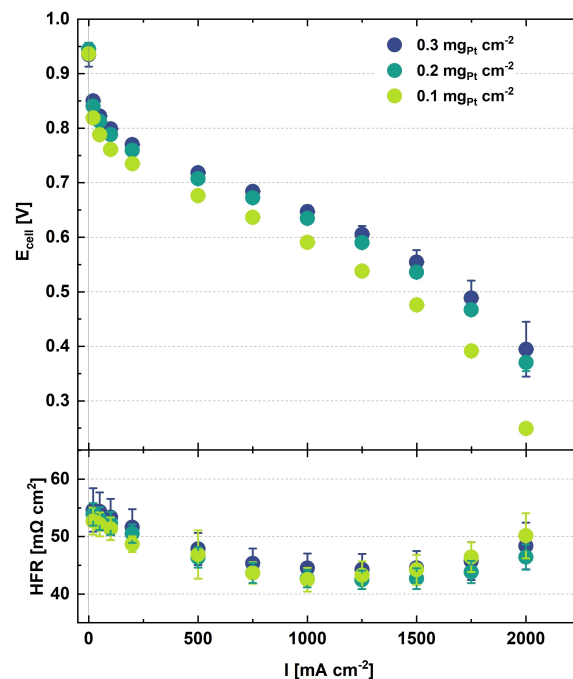


Figure 5. Polarization curve of all three measured cathode loadings of the three coating repetitions at 80°C , 95% relative humidity with a N211 membrane and an anode loading of $0.11 \text{ mg}_{\text{Pt}} \text{ cm}^{-2}$. The anode was fed with $0.25 \text{ ml min}^{-1} \text{ H}_2$ and the cathode with $0.75 \text{ ml min}^{-1} \text{ air}$. The bottom panel shows their measured HFR values. All displayed curves show the mean values of the three measurements for each loading and the error bars indicate the standard deviation.

The HFR corrected I–V-curve, the measured crossover current, resistance for the electrical short, protonic sheet resistance and ECSA can be found in the supporting information (S3)

Conclusions

We presented a tabletop R2R slot die setup for producing graded catalyst layers for electrochemical systems. Via the variation of the volume flow into the slot die head we manufactured a wet film graded catalyst layer for PEMFC. The wet film thickness was measured in-line. The XRF Pt Intensity and the gravimetric loading were determined. All three values correlated linearly with each other. The full cell PEMFC tests of the different cathode loadings showed consistency with results of what was reported in literature so far. In summary the setup is a robust option for conducting screening of different loadings via graded catalyst slot die coatings. Further loading study experiments for other electrochemical systems or new catalysts will be carried out in the future. Further developments will be conducted to allow two ink experiments for enabling advanced studies of for instance the I/C ratio via one graded catalyst coating. Additionally, the gained results can be applied in a graded catalyst layer on a CCM in a stack application for performance increase when using a wider slot die head. For future applications, a better understanding of the behaviour of

the ink during the coating process and improved analysis, as XRF calibration, will be required.

Author Contributions

George Pätzold: Conceptualization (equal), Data Curation (lead), Formal analysis (lead), Investigation (lead), Methodology (lead), Validation (lead), Visualization (lead), Writing – Original Draft Preparation (lead), Writing – Review & Editing (equal). Maximilian Maier: Formal Analysis (support), Investigation (support), Writing – Review & Editing (equal). Lukas Löttter: Formal Analysis (support), Investigation (support), Writing – Review & Editing (equal). Anna T. S. Freiberg: Conceptualization (equal), Funding Acquisition (supporting), Writing – Review & Editing (equal). Simon Thiele: Conceptualization (equal), Funding Acquisition (lead), Supervision (equal), Writing – Review & Editing (equal). Dominik Dworschak: Conceptualization (equal), Project Administration (lead), Supervision (equal), Writing – Review & Editing (equal).

Acknowledgements

We thank the German Federal Ministry of Education and Research (BMBF) for the financial support in the HyThroughGen Project (03HY108A), Julian Grüber for support of the visualisation of the R2R setup in a schematic drawing and Marc Ayoub and Andreas Bösmann for advice with SEM and XRF analysis, respectively. Open Access funding enabled and organized by Projekt DEAL.

Conflict of Interests

The authors declare no conflict of interests

Data Availability Statement

The data that support the findings of this study are available from the corresponding author upon reasonable request.

Keywords: catalyst loading • fuel cells • high-throughput screening • in-plane gradient • R2R

- [1] I. Staffell, D. Scamman, A. Velazquez Abad, P. Balcombe, P. E. Dodds, P. Ekins, N. Shah, K. R. Ward, *Energy Environ. Sci.* **2019**, *12*, 463.
[2] S. Khandavalli, J. H. Park, N. N. Kariuki, D. J. Myers, J. J. Stickel, K. Hurst, K. C. Neyerlin, M. Ulsh, S. A. Mauger, *ACS Appl. Mater. Interfaces* **2018**, *10*, 43610.

- [3] F. L. Deschamps, J. G. Mahy, A. F. Léonard, S. D. Lambert, A. Dewandre, B. Scheid, N. Job, *Thin Solid Films* **2020**, *695*, 137751.
[4] R. Alink, R. Singh, P. Schneider, K. Christmann, J. Schall, R. Keding, N. Zamel, *Molecules* **2020**, *25*, 1523.
[5] A. M. Chaparro, B. Gallardo, M. A. Folgado, A. J. Martín, L. Daza, *Catal. Today* **2009**, *143*, 237.
[6] P. Schneider, M. Batool, A. O. Godoy, R. Singh, D. Gerteisen, J. Jankovic, N. Zamel, *J. Electrochem. Soc.* **2023**, *170*, 24506.
[7] T. Schuler, A. Chowdhury, A. T. Freiberg, B. Sneed, F. B. Spingler, M. C. Tucker, K. L. More, C. J. Radke, A. Z. Weber, *J. Electrochem. Soc.* **2019**, *166*, F3020–F3031.
[8] J. P. Owejan, J. E. Owejan, W. Gu, *J. Electrochem. Soc.* **2013**, *160*, F824–F833.
[9] L. Hao, K. Moriyama, W. Gu, C.-Y. Wang, *J. Electrochem. Soc.* **2015**, *162*, F854–F867.
[10] Y. Guo, F. Pan, W. Chen, Z. Ding, D. Yang, B. Li, P. Ming, C. Zhang, *Electrochem. Energy Rev.* **2021**, *4*, 67.
[11] A. Orfanidi, P. J. Rheinländer, N. Schulte, H. A. Gasteiger, *J. Electrochem. Soc.* **2018**, *165*, F1254–F1263.
[12] G. S. Harzer, J. N. Schwämmlein, A. M. Damjanović, S. Ghosh, H. A. Gasteiger, *J. Electrochem. Soc.* **2018**, *165*, F3118–F3131.
[13] I. Fouzaï, S. Gentil, V. C. Bassetto, W. O. Silva, R. Maher, H. H. Girault, *J. Mater. Chem. A* **2021**, *9*, 11096.
[14] a) M. Wagner, A. Distler, V. M. Le Corre, S. Zapf, B. Baydar, H.-D. Schmidt, M. Heyder, K. Forberich, L. Lüer, C. J. Brabec et al., *Energy Environ. Sci.* **2023**, *16*, 5454; b) S. Moradi, S. Kundu, M. Rezazadeh, V. Yeddu, O. Voznyy, M. I. Saidaminov, *Commun. Mater.* **2022**, *3*, 13; c) S. Moradi, S. Kundu, M. Awais, Y. Haruta, H.-D. Nguyen, D. Zhang, F. Tan, M. I. Saidaminov, *Small (Weinheim an der Bergstrasse, Germany)* **2023**, *19*, 2301037; d) S. Moradi, *Dissertation*, University of Victoria, Victoria, **2023**; e) T.-J. Jeong, X. Yu, T. A. L. Harris, *ACS Appl. Mater. Interfaces* **2024**, *16*, 9264; f) J. Alstrup, M. Jørgensen, A. J. Medford, F. C. Krebs, *ACS Appl. Mater. Interfaces* **2010**, *2*, 2819.
[15] M. Ayoub, T. Böhm, M. Bierling, S. Thiele, M. Brodt, *J. Electrochem. Soc.* **2024**, *171*, 94503.
[16] a) S. Herden, F. Riewald, J. A. Hirschfeld, M. Perchthaler, *J. Power Sources* **2017**, *355*, 36; b) S.-Y. Lee, H.-J. Kim, K.-H. Kim, E. CHO, I.-H. Oh, T.-H. Lim, *Electrochem. Solid-State Lett.* **2007**, *10*, B166; c) M. Prasanna, E. A. Cho, H.-J. Kim, I.-H. Oh, T.-H. Lim, S.-A. Hong, *J. Power Sources* **2007**, *166*, 53; d) M. Santis, S. A. Freunberger, A. Reiner, F. N. Büchi, *Electrochim. Acta* **2006**, *51*, 5383; e) L. Xing, Y. Wang, P. K. Das, K. Scott, W. Shi, *Chem. Eng. Sci.* **2018**, *192*, 699; f) L. Xing, Y. Xu, Z. Penga, Q. Xu, H. Su, F. Barbir, W. Shi, J. Xuan, *Chem. Eng. J.* **2021**, *406*, 126889; g) Y. Zhang, A. Smirnova, A. Verma, R. Pitchumani, *J. Power Sources* **2015**, *291*, 46.
[17] a) X. Zhang, H. Li, J. Yang, Y. Lei, C. Wang, J. Wang, Y. Tang, Z. Mao, *RSC Adv.* **2021**, *11*, 13316; b) R. L. Borup, A. Kusoglu, K. C. Neyerlin, R. Mukundan, R. K. Ahluwalia, D. A. Cullen, K. L. More, A. Z. Weber, D. J. Myers, *Curr. Opin. Electrochem.* **2020**, *21*, 192.
[18] C. van Pham, D. Escalera-López, K. Mayrhofer, S. Cherevko, S. Thiele, *Adv. Energy Mater.* **2021**, *11*, 2101998.
[19] N. Du, C. Roy, R. Peach, M. Turnbull, S. Thiele, C. Bock, *Chem. Rev.* **2022**, *122*, 11830.
[20] R. Makharia, M. F. Mathias, D. R. Baker, *J. Electrochem. Soc.* **2005**, *152*, A970.
[21] J. Landesfeind, J. Hattendorff, A. Ehrl, W. A. Wall, H. A. Gasteiger, *J. Electrochem. Soc.* **2016**, *163*, A1373–A1387.
[22] T. A. Greszler, D. Caulk, P. Sinha, *J. Electrochem. Soc.* **2012**, *159*, F831–F840.
[23] M. Maier, D. Abbas, J. Mitrovic, A. Marth, S. Thiele, T. Böhm, *ACS Appl. Energy Mater.* **2024**, *7*, 10637.
[24] D. Gerteisen, N. Zamel, C. Sadeler, F. Geiger, V. Ludwig, C. Hebling, *Int. J. Hydrogen Energy* **2012**, *37*, 7736.

Manuscript received: December 13, 2024
Revised manuscript received: February 28, 2025
Version of record online: March 12, 2025